Journal of Sustainable Development of Energy, Water and Environment Systems

http://www.sdewes.org/jsdewes

Year 2027, Volume 15, Issue 1, 1140783

Original Research Article

Open access

An Adaptive Perturb and Observe Maximum Power Point Tracking Algorithm with Dead-Band Control for Photovoltaic Systems Under Rapid Irradiance Changes

Krismadinata Krismadinata*[*1], Asnil Asnil[1], Ricky Maulana[1], Refdinal Nazir[2], Muhammad Nasir Sonni[2], Jeyraj Selvaraj[3]

[1]Department of Electrical Engineering, Faculty of Engineering, Universitas Negeri Padang, Padang 25131, Indonesia

[2]Department of Electrical Engineering, Faculty of Engineering, Universitas Andalas, Padang 25163, Indonesia

[3]UMPEDAC, University of Malaya, Kuala Lumpur, Malaysia

e-mail: krisma@ft.unp.ac.id; asnil81@ft.unp.ac.id; ricky.maulana@ft.unp.ac.id, refdinalnazir@eng.unand.ac.id; m.nasir.sonni@eng.unand.ac.id jeyraj@um.edu.my

Cite as: Krismadinata, K., Asnil, A., Maulana, R., Nazir, R., Sonni, M. N., Selvaraj, J., An Adaptive Perturb and Observe Maximum Power Point Tracking Algorithm with Dead-Band Control for Photovoltaic Systems Under Rapid Irradiance Changes, J.sustain. dev. energy water environ. syst., 15(1), 1140783, 2027, DOI: https://doi.org/10.13044/j.sdewes.d14.0783

ABSTRACT

The conventional technique for tracking the maximum power point based on Perturb and Observe remains widely used because of its ease of implementation. However, it often suffers from sustained power oscillation and poor tracking accuracy under rapidly varying irradiance conditions. This paper proposes an Optimized Adaptive Perturb and Observe system that addresses these limitations by integrating a slope-dependent variable step size method with dead-band control. During environmental transients, the adaptive variable step size responds to the power-voltage curve gradient to accelerate maximum power point tracking, whereas in the quiescent phase, the dead-band threshold stabilizes the duty cycle under small power variations, thereby suppressing undesirable oscillations. Hardware-in-the-loop validation using a boost converter shows that the proposed system reduces stabilization time from 115 ms to 60 ms, nearly eliminates the 6.5 W steady-state ripple, increases total power yield by 12.2%, and remains suitable for commercial-scale photovoltaic systems due to its low computational demand.

KEYWORDS

Maximum power point tracking, Perturb and observe, Variable step size, Dead-band control, Photovoltaic systems.

* Corresponding author

Submitted 26.04.2026; Revised 26.09.2026; Accepted 14.10.2026; Available online 23.11.2026.

Copyright: © 2026 The Author(s). *JSDEWES*, published by SDEWES Centre, Zagreb, Croatia. This article is an open access article distributed under the terms and conditions of the Creative Commons Attribution 4.0 International License (CC BY 4.0)

INTRODUCTION

The global expansion of photovoltaic (PV) installations reflects the increasing role of solar energy in the transition toward cleaner and more sustainable power systems [1]. However, the electrical output of a PV array is highly sensitive to environmental variations, particularly irradiance and temperature, which continuously shift the operating point away from the maximum power point (MPP) [2]. Therefore, maximum power point tracking (MPPT) remains an important function in PV energy conversion systems, as it directly affects the energy harvesting efficiency, system response, and practical feasibility of PV applications under dynamic operating conditions [3].

Among the many MPPT techniques reported in the literature, Perturb and Observe (P&O) remains one of the most widely used approaches due to its simple structure, easy implementation and low computational burden, which make it attractive for low-cost embedded applications [4]. But the standard P&O algorithm has two disadvantages. Firstly, the use of a fixed perturbation step introduces an intrinsic trade-off between transient speed and steady-state performance [5]. A large step size increases the speed of convergence towards the MPP with a larger oscillation around the operating point. A small step size reduces the oscillation but decreases the speed of the tracking response [6]. Secondly, the classical P&O decision logic is likely to confuse power variations due to environmental conditions with those of its own perturbation for rapidly changing irradiance, causing a tracking drift and departure from the actual MPP [7]. These disadvantages reduce the total harvested energy, especially for applications under frequent irradiance transitions.

A lot of modified P&O-based MPPT methods have been proposed in recent years to cope with these limitations [8]. The first group of studies concerns on the strategies based on variable step size (VSS) where the perturbation magnitude is adaptively adjusted to obtain a better trade-off between convergence speed and steady-state oscillation [9]. Although these methods generally improve dynamic response, many of them still show residual oscillation near the MPP, particularly under rapidly changing irradiance [10]. The second group addresses drift via modified decision logic [11], correction mechanisms [12], current-based perturbation or model-based formulations [13]. These methods can improve the accuracy of transient tracking but usually at the expense of increased logic, increased implementation complexity, or decreased practicality for low-cost controllers. The third group consists of hybrid and intelligent MPPT methods including fuzzy-based [14], neural-network-based [15], voltage scanning [16], modified coot optimization algorithm [17], and optimization-assisted methods [18]. These methods can track very well, but are normally more computationally demanding and so less attractive when the main design requirements are simplicity of implementation, transparency and robustness in a real-time system.

From a practical implementation perspective, an important gap therefore remains. Existing VSS-based methods improve convergence speed, but often do not sufficiently suppress oscillation around the MPP under rapidly varying irradiance [19]. In contrast, methods developed to mitigate drift during irradiance transitions frequently rely on more elaborate control logic or additional computational burden [20]. Consequently, few low-complexity and hardware-validated adaptive P&O methods simultaneously provide fast transient response, reduced steady-state oscillation, and numerically robust operation under rapidly varying uniform irradiance conditions. For practical PV systems, such a combination is important because improved MPPT stability not only enhances instantaneous tracking accuracy but also contributes to more effective energy harvesting over time. A concise summary of the literature gap and the positioning of the proposed method is presented in **Table 1**.

In order to fill this gap this paper suggests an Optimised Adaptive P&O (OA-P&O) MPPT algorithm for PV systems under rapidly changing uniform irradiance. The proposed method

combines a slope-based VSS mechanism with dead-band stabilization in a low-complexity framework. The perturbation step is adaptively adjusted during irradiance changes based on the slope of the *P-V* characteristic to speed up convergence to the MPP. Near steady state operation, a dead-band mechanism suppresses unnecessary duty cycle perturbations, leading to a reduction of oscillation around the operating point. Further, a bounded slope calculation strategy is proposed to avoid unstable updates in the case of near-zero voltage variation, which enhances computational robustness for small-signal operating conditions.

Table 1. Summary of the literature gap and positioning of the proposed OA-P&O method

Method category	Representative references	Core idea	Drift mitigation	Oscillation reduction near MPP	Hardware / real-time validation	Relative complexity	Main limitation
Conventional P&O	[21], [22]	Fixed-step perturbation based on power response	No	No	Yes, widely used in practice	Low	Simple and practical, but suffers from the speed–oscillation trade-off and drift under rapidly varying irradiance
Adaptive / VSS-based P&O	[18], [23], [24]	Perturbation step is adjusted according to operating conditions or PV curve information	Partial / indirect	Partial	Sometimes	Low–Medium	Improves dynamic response, but residual oscillation may still remain near the MPP, especially during rapid irradiance changes
Drift-mitigation / drift-avoidance P&O variants	[7], [25]	Modified decision logic, correction terms, current perturbation, or model-assisted update to reduce tracking drift	Yes	Partial	Limited / method-dependent	Medium	Better transient robustness, but often requires additional logic, model dependence, or higher implementation effort

Method category	Representative references	Core idea	Drift mitigation	Oscillation reduction near MPP	Hardware / real-time validation	Relative complexity	Main limitation
Hybrid / intelligent MPPT methods	[15], [26]–[28]	Fuzzy, ANN, optimization, or hybrid search strategies	Yes	Yes	Limited / selective	Medium–High to High	Strong tracking capability, but computational burden, tuning effort, and reduced implementation simplicity may limit practical deployment
Proposed OA-P&O	This work	Slope-based variable step size combined with dead-band stabilization and bounded slope computation	Yes (practical mitigation)	Yes	Yes (hardware-in-the-loop)	Low	Designed to preserve implementation simplicity while improving transient speed, steady-state stability, and numerical robustness under rapidly varying uniform irradiance

This work has contributions in the development of a low-complexity adaptive P&O structure that integrates slope-based VSS and dead-band stabilisation for fast irradiance transitions, designing a bounded slope computation strategy for stable update behaviour under very small voltage variations, and hardware-in-the-loop validation of the proposed OA-P&O method under rapidly varying uniform irradiance. The proposed method has been shown to produce faster stabilisation, reduced steady-state oscillation, and higher harvested power than the classic P&O algorithm, while being simple to apply for actual PV systems.

BACKGROUND AND PROPOSED ALGORITHM

This section establishes the theoretical background and structure of the proposed MPPT system. It begins by evaluating the operational mechanics and key limitations of the conventional perturb and observe method under dynamic irradiance. It then outlines the core design of the optimised adaptive perturb and observe algorithm, followed by a detailed discussion of the slope-bounded calculation and dead-band stabilization mechanisms that ensure numerical stability and operational robustness.

Conventional Perturb and Observe (P&O)

The conventional P&O approach on analyzing power variations relative to incremental voltage changes. As demonstrated in [29], its inability to separate environmental fluctuations from resulted from control process often leads to instability and drift under dynamic irradiation. The approach works by effectively comparing the current power output $P(k)$ to the previous measurement $P(k\text{-}1)$. If the power is increasing it means that the system is approaching to the maximum point and the adjustments will stay in the same direction. If the power is decreasing the direction of perturbation must be changed to stay on the MPP [30].

The main drawback of this approach is the oscillation under steady-state conditions. Another important shortcoming is the occurrence of drift phenomena when solar irradiance levels increase rapidly [31]. This approach also cannot distinguish the isolation changes, resulting in the displacement of the operating trajectory from the true MPP [32].

Optimize Adaptive P&O (OA-P&O) Algorithm

The OA-P&O algorithm in this work is designed with three main objectives: (1) eliminating steady-state oscillations near the MPP; (2) reducing drift during rapid irradiance changes without additional sensors; and (3) ensuring computational robustness under low voltage variation conditions. The VSS implementation in this algorithm is based on an enhanced single slope. The VSS logic is divided based on the power change threshold, ε (epsilon), to achieve an appropriate balance between tracking speed and system stability, as shown in the flowchart in Figure 1.

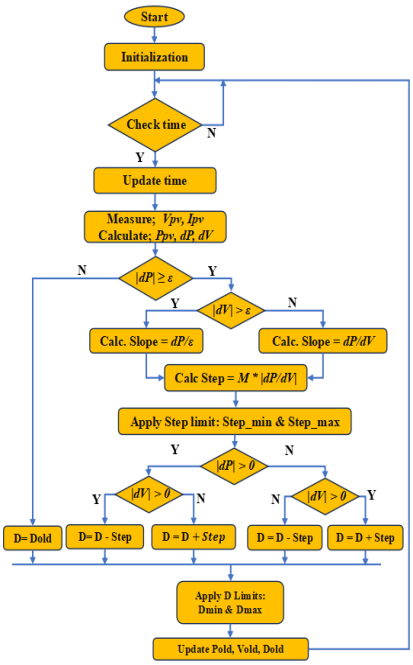


Figure 1. The proposed algorithm

The suggested OA-P&O method is shown in Figure 1. The proposed algorithm and is designed to function in two different modes: a dynamic mode for fast tracking and a stagnant mode which serves as a dead-band stability mechanism. If the absolute change in power $|\Delta P|$ is greater than or equal to the error threshold ε ($|\Delta P| \geq \varepsilon$), the operating point is considered far from the MPP and the controller switches to dynamic mode. In this manner the perturbation step size is obtained by utilising a variable step-size (VSS) formulation proportional to the local gradient of the P–V characteristic as indicated in eq. (1) [33] :

$$Step = M \times \left|\frac{\Delta P}{\Delta V}\right| \quad (1)$$

where M is a positive scale factor that regulates the sensitivity of the adaptive step size, ΔP is the power fluctuation between two sampling instants and ΔV is the corresponding voltage change. This formulation allows a higher step size at a relatively far operating point from the MPP (the P-V curve is steeper), thus accelerating convergence. When the operating point is closer to MPP and its slope is modest, the perturbation step is reduced automatically. This avoids overshoot and large oscillations about the operating point.

As ΔV approaches 0, practical issues arise in slope-based adaptive systems. This can occur during steady-state operation or because of limitations in sensor resolution. Direct evaluation of $\Delta P/\Delta V$ under these conditions can yield step values that are too big or numerically unstable. The proposed OA-P&O method recognises this case and manages it by swapping ε for ΔV. It guarantees bounded step-size computation and enhances numerical resilience of the controller without requiring additional sensors or a high-end estimation approach.

The controller enters into stagnant mode if the absolute change in power is less than a threshold, i.e., $|\Delta P| < \varepsilon$. In this mode, the operating point is deemed to be close enough to the MPP, and superfluous duty-cycle disturbances are suppressed. A dead-band action is implemented to eliminate repetitive minor disturbances which do not contribute much to tracking improvement but may cause a large rise in steady-state ripple. Therefore, the stagnant mode stabilises the duty cycle for small power change and enhances the steady-state performance by decreasing the oscillation around the MPP.

The suggested OA-P&O algorithm improves the existing P&O approach in two complementary ways. First, it enhances transient tracking performance via slope-based adaptive perturbation under fast-varying irradiance conditions. Secondly, it enhances the steady-state stability by dead-band-assisted oscillation suppression and bounded slope evaluation. The controller thus retains the simple structure of the classic P&O technique but with enhanced tracking speed, smaller ripple, and better robustness in the case of fast shifting uniform irradiance.

Optimization and Robustness

The main advantage of the proposed OA-P&O algorithm lies not only the dual-mode variable step-size feature but also in the systematic determination of key control parameters controlling system stability and dynamic tracking response. The algorithm is designed in a coordinated way to ensure reliable operation under fluctuating atmospheric conditions while preserving steady-state stability around the MPP.

A major aspect of this robustness lies in the computation of the adaptive step size. In slope-based VSS systems, numerical instability arises from the expression $\Delta P/\Delta V$ if the voltage variation $|\Delta V|$ approaches zero during stead-state operation or sensor resolution limits. The proposed OA-P&O addresses this problem by integrating a division-by-zero prevention technique directly into the control execution flow. To eliminate mathematical ambiguity, the controller utilizes two distinct, empirically determined parameters: a voltage singularity threshold $(\varepsilon_{\mathrm{v}})$ and power dead-band threshold $\left(\epsilon_{\mathrm{p}}\right)$. When $|\Delta V| < \varepsilon_{\mathrm{v}}$, the denominator in the slope calculation is constrained to ε_{v}, yielding the bounded computation $\frac{\Delta P}{\varepsilon_{\mathrm{v}}}$. This adjustment prevents numerical singularity and ensures controller stability during online execution. On the power side, the dead-band threshold ϵ_{p} represents the minimal observable power variation above system noise. The controller enters dead-band mode when $|\Delta P| < \epsilon_{\mathrm{p}}$, suppressing duty-cycle perturbations too reduce steady-state oscillations around the MPP.

To ensure operational reliability across dynamic environments, the control parameters namely ε_{v}, ϵ_{p}, and the scaling factor M were determined through empirical, hardware constrained tuning matched to the signal acquisition setup. Both ε_{v}, and ϵ_{p} where selected based on the measured noise floor and ADC quantization resolution of the voltage and current

sensing circuits. Setting these thresholds too high degrades tracking sensitivity, whereas setting them too low allows high frequency noise to trigger unnecessary step updates.

Meanwhile, the scaling factor M governs the slope-dependent step size. A large M accelerates transient convergence toward the MPP during rapid irradiance changes but can increase initial overshoots. Conversely, a smaller M offers smoother transitions profiles at the expense of tracking speed. A sensitivity trade-off analysis guided the selection of M, ensuring rapid perturbation scaling during large gradients $\left(\frac{\Delta P}{\Delta V}\right)$ while smoothly decaying as the operating point nears the MPP prior to triggering the dead-band mode $(|\Delta P| < \varepsilon)$. Furthermore, the MPPT update interval was chosen to balance dynamic responsiveness and noise filtering, mitigating drift under rapidly changing environments without increasing algorithm complexity.

DC-DC BOOST CONVERTER IMPLEMENTATION

In this section, the DC–DC boost converter used as the power interface for implementing and validating the proposed OA-P&O MPPT algorithm is discussed. The DC-DC boost converter is designed in such a way that it can provide stable operation, sufficient voltage gain, and fast dynamic response, so that the improvements in performance can be mainly due to the MPPT algorithm and not due to the limitations of the DC-DC boost converter. The adjustment of the PV operating point to the MPP is typically performed by a DC-DC converter interface [34]. Among the various options, the most commonly used MPPT device is the DC-DC boost converter [35]. Its main utility lies in its ability to synchronize the input impedance with the dynamic characteristics of the PV array while simultaneously boosting the voltage for end-use applications like grid connection. Moreover, the tracking process is realized by using duty cycle as a fundamental control input, allowing for continuous adjustment of the input voltage to match the target set by the MPPT algorithm.

The boost converter stage comprising an inductor, a MOSFET power switch, a fast-recovery diode, and filtering capacitors is integrated directly into the overall experimental setup depicted in Figure 2. Component values were calculated using the standard design equations given in eqs. (2)-(5) [36].

$$\frac{V_{\text{out}}}{V_{\text{pv}}} = \frac{1}{1-D} \tag{2}$$

$$C_1 \geq \frac{D}{8 \times f^2 \times L \times \Delta V_{\text{in}}} \tag{3}$$

$$C_2 \geq \frac{D}{f \times R \times \Delta V_{\text{out}}} \tag{4}$$

$$L = \frac{D \times (1\text{-}D)^2 \times R}{r \times f} \tag{5}$$

Based on eqs. ((2)-((5), the component value for the boost converter is obtained as presented in Table 2. Some of the value used in the boost converter hardware, as shown in Table 2 , are the result of optimization adjusted to safety margin of commercially available components.

Table 2. Boost converter parameter values

No	Parameter	Value
1	Input voltage	36.2 V
2	Duty cycle	0.6
3	Output voltage	90.5 V
4	Frequency	20 kHz
5	Input capacitor	100 µF
6	Output capacitors	100 µF
7	Inductor	2.2 mH
8	MOSFET	IRFP460
9	Diode	MUR1560G
10	Resistor	70 Ohm

The objective of determining the specifications of the components is to realize satisfactory voltage amplification, reduce ripple, and high operational threshold across all test conditions of irradiance. In addition, inductance value and capacitance rating are specified to realize the Continuous Conduction Mode (CCM) with reduced input voltage fluctuations, which is important for voltage sensing stability.

The boost converter will be controlled to operate in CCM with a switching frequency set to 20 kHz. This ensures a transient response that will be considerably faster than one obtained by the MPPT's sampling frequency. Hence, the boost converter's response will not be a bottleneck for the tracking performance, validating the improvement achieved by the proposed OA-P&O logic.

EXPERIMENTAL SETUP

The experimental setup was developed to evaluate the real-time performance of the proposed OA-P&O algorithm under rapidly varying uniform irradiance conditions and to compare it fairly with the conventional P&O method. The test platform consists of a PV source, a boost converter, a controller implementation unit and measuring devices to record the electrical response of the system.

Figure 2 shows the overall setup of the MPPT test bench.

In the test platform, the PV source is connected to a boost converter that serves as the power-conditioning stage. The converter provided a controllable interface between the PV module and the load, allowing the MPPT to control the operating point by duty-cycle adjustment. **Table 2** shows the converter settings. This arrangement is used in order to make the measured response represent the performance of the MPPT algorithm under actual operating conditions and to simulate a practical PV energy conversion system.

Furthermore, the controller is developed in real time and programmed to perform the MPPT updating procedure based on the measured PV voltage and current signals. From these signals, the instantaneous power was estimated, and the associated values of ΔP and ΔV are used for the determination of the perturbation step according to the selected algorithm. The suggested OA-P&O used the adaptive step-size logic, bounded slope calculation, and dead-band mode, as mentioned in the previous section. For comparison, the typical P&O algorithm is implemented on the same platform with the identical sensing signals, converter, switching conditions, and test scenarios.

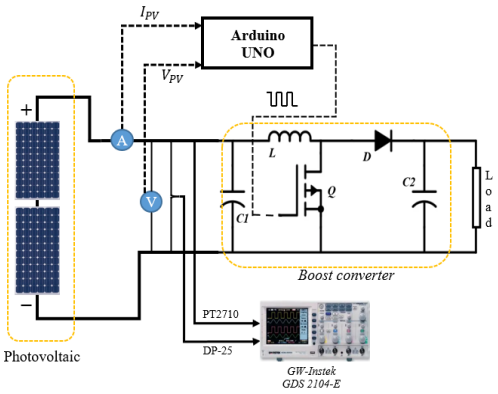


Figure 2. Block diagram of the MPPT system testing

This experiment is conducted under laboratory conditions so that natural sunlight is emulated using thirty-six halogen lamps, each rated at 150 W. **Figure 3** shows how six sets of halogen lamps are organized to provide controlled fluctuations of irradiance. The switching and management of these lamp groups was adapted to the irradiance patterns summarised in **Table 3**. This configuration allowed several tests at varying irradiance levels and quick environmental transitions, giving a controlled framework for the assessments of the tracking behaviour of both the standard P&O and the suggested OA-P&O algorithms.

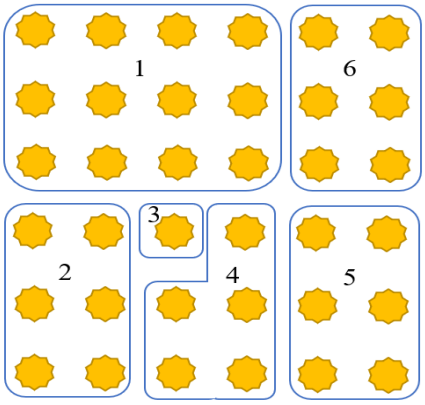


Figure 3. Halogen lamp grouping for illumination variation

Table 3. Halogen lamp configuration

Pattern	**Halogen lamp**					
	Group 1	Group 2	Group 3	Group 4	Group 5	Group 6
I	ON	ON	ON	ON	OFF	OFF
II	ON	ON	ON	ON	ON	ON
III	OFF	OFF	OFF	OFF	ON	ON
IV	ON	ON	OFF	OFF	ON	ON

These irradiance variation profiles are utilized to characterize abrupt environmental transitions as well as near-steady-state operational regions. Both algorithms are tested under the same operational conditions for each test pattern. The methodology is constructed to assess the tracking capabilities, steady state stability, and robustness of each approach consistently

and reliably. The experimental hardware used for validation is shown in **Figure 4**. It consists of the halogen lamp array, boost converter, controller platform, and measurement equipment.

Some of the variables are captured during the tests including PV voltage, PV current, output power, tracking response and ripple behaviour near steady state operation. The experiments are conducted and compared for the stabilisation time, steady-state oscillations and harvested power for the applied irradiation pattern. The implemented setting, with the real-time implementation and the controlled variations of the irradiance, provides a reliable base for the assessment of the practical efficiency of the proposed OA-P&O method.

RESULT AND DISCUSSION

This section discusses the experimental validation of the proposed OA-P&O algorithm and compares it with the conventional P&O approach under the same laboratory settings. The evaluation is made on the basis of three key performance indicators, including harvested power, steady-state oscillation and transient tracking speed. **Figure 4** experimental hardware designed based on the schematic of the converter illustrated in

Figure 2. The same platform was used to evaluate the practical MPPT performance of both controllers under identical working conditions. The measured dynamic responses of the traditional P&O and the suggested OA-P&O are shown in **Figure 5** and **Figure 6**, respectively, and the relevant steady-state and transient performance parameters are summarised in **Table 4** to **Table 7**. Besides the comparison of the numerical results, this part analyses the contribution of the adaptive variable step-size mechanism and dead-band operation to the observed improvement in the tracking accuracy, oscillation suppression and power extraction capabilities.



Figure 4. Experimental hardware (solar simulator, converter, and measurement equipment)

Performance of Conventional Perturb & Observe (P&O)

Figure 5 shows the experimental response of the conventional P&O algorithm for the irradiance variation patterns studied in this work. The baseline method fulfils its purpose of tracking, as a general rule, the controller is capable of moving the operating point in the neighbourhood of the MPP, after each variation of irradiance. However, the measured waveforms also demonstrate an obvious limitation of the fixed-step perturbation strategy, particularly when the operating point is near the steady-state operation. The controller keeps disturbing the duty cycle instead of a smooth settling. This creates repetitive volatility in the output response.

The quantitative results summarised in **Table 4** support this behaviour. The worst deficiency of the studied patterns is found in pattern II with a power ripple of 6.5 W. This finding implies that the fixed perturbation step still works when the operating point is near the MPP, resulting in undesirable oscillation around the optimal zone. This perturbation is intrinsic

to the conventional P&O principle. However, its practical result is a decrease in the energy extraction efficiency since a part of the working time is spent away from the genuine maximum power point. The voltage and current responses likewise exhibit limiting ripple behaviour, suggesting that the constraint is structural rather than incidental.

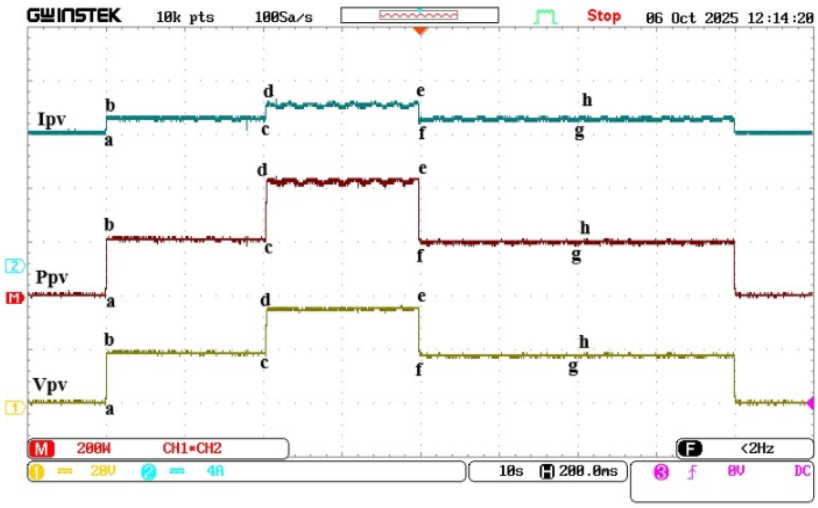


Figure 5. The performance of the conventional P&O MPPT algorithm with the outputs is Vpv, Ppv, and Ipv (scale 10s/div; Vpv (Ch1) 20V/div; Ipv (Ch2) 4A/div; and Ppv (math trace) 200 W/div)

Table 4. The measured of Voltage, current, power ouput, and oscillation steady state condition using P&O algorithm

Pattern	**Photovoltaic Output**			**Oscillation steady state**		
	Voltage [A]	Current [V]	Power [W]	Voltage [V]	Current [mA]	Power [W]
I	19.01	0.951	18.09	ND	ND	ND
II	35.44	1.984	70.31	ND	560	6.5
III	18.11	0.916	16.59	ND	320	NA
IV	18.15	0.915	16.61	ND	320	NA

ND: not detected within the measurement resolution of the data acquisition system.

The transient tracking performance of the conventional P&O is summarized in **Table 5**. The slowest response is observed during the c-to-d transition, where the power signal requires 115 ms to stabilize. The e-to-f transition also shows a relatively long stabilization time of 90 ms. These results reveal the well-known trade-off of fixed-step P&O control: a perturbation step that is sufficiently large to ensure acceptable transient motion may still be too large for steady-state operation, thereby causing persistent oscillation after convergence. Therefore, while the conventional P&O remains attractive because of its simplicity and low implementation cost, the experimental results confirm that its fixed-step structure limits both steady-state stability and transient responsiveness under rapidly varying irradiance conditions.

Table 5. Tracking speed metric of using P&O algorithm

Transition	**Tracking speed [ms]**		
	Voltage signal	Current signal	Power signal
a to b	85	83	85
c to d	115	80	115
e to f	80	70	90
g to h	ND	ND	ND

ND: not detected within the measurement resolution of the data acquisition system.

The limitations observed in the conventional P&O results provide the experimental basis for evaluating whether the proposed OA-P&O can improve both dynamic tracking and steady-state stability through its adaptive step-size and dead-band mechanisms.

Performance of the Proposed OA-P&O Algorithm

The operational results of the introduced OAP&O MPPT schema are illustrated in **Figure 6** which demonstrates a significant suppression of steady-state ripples. In contrast to the conventional P&O method, the measured waveforms show a smoother transition toward the operating point and a more stable behaviour once the system approaches the MPP. This response indicates that the proposed controller is able to adapt its perturbation action according to the operating condition, allowing faster correction during irradiance transitions while avoiding unnecessary fluctuations near steady state. As a result, the overall tracking behaviour becomes more consistent under varying operating conditions.

The steady-state performance of the proposed OA-P&O is given in **Table 6**. The proposed controller clearly shows the reduction of oscillatory behaviour around the MPP with respect to the existing technique. The results show that no quantifiable steady-state ripple found for the investigated patterns. It indicates that the dead-band mechanism successfully suppresses unnecessary duty-cycle perturbations when the power fluctuation is considered small. This behaviour is important because it allows the controller to remain close to the maximum power region without continuously forcing the operating point to move around it. The increase in measured output power across all test patterns also indicates that ripple reduction directly contributes to increased energy harvesting.

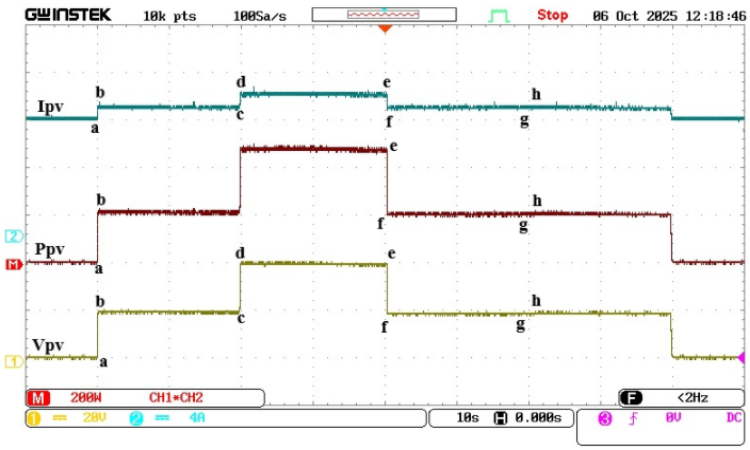


Figure 6. Performance of the OA-P&O MPPT algorithm with the outputs is Vpv, Ppv, and Ipv (scale: 10 s/div; Vpv (Ch1) 20 V/div; Ipv (Ch2) 4 A/div; and Ppv (math trace) 200 W/div)

Table 6. The measured of voltage, current, power ouput, and oscillation steady state condition using OA-P&O algorithm

Pattern	Photovoltaic Output			Oscillation steady state		
	Voltage [A]	Current [V]	Power [W]	Voltage [V]	Current [mA]	Power [W]
I	19.59	1.108	21.71	ND	ND	ND
II	40.26	1.959	78.87	ND	ND	ND
III	18.89	1.050	19.83	ND	ND	ND
IV	18.91	1.049	19.84	ND	ND	ND

ND: not detected within the measurement resolution of the data acquisition system.

The transient performance of the proposed OA-P&O is further presented in **Table 7**. The tracking speed time indicate that the controller exhibits a faster response than the conventional P&O during irradiance transitions, particularly for the most challenging operating adjustments. The improvement is related to the adaptive VSS mechanism which enhances the step of the perturbation when the operating point is far from the MPP and diminishes it when the operating point is near the optimum region. Therefore, the suggested controller boosts the convergence speed without losing the steady-state stability. The experimental results show that the OA-P&O algorithm provides a more balanced MPPT behaviour, combining a faster transient tracking with a reduction of the steady-state oscillations.

Table 7. Tracking speed metric of using OA-P&O algorithm

Transition	Tracking speed [ms]		
	Voltage signal	Current signal	Power signal
a to b	80	60	80
c to d	100	65	90
e to f	60	55	60
g to h	ND	ND	ND

ND: not detected within the measurement resolution of the data acquisition system.

Comparative Performance Analysis

A direct comparison between the conventional P&O and the proposed OA-P&O shows that the benefits of the proposed method are not limited to a specific performance parameter. Instead, the experimental results demonstrate a simultaneous improvement in both the harvested power and the transient response. The OA-P&O controller is proven to be capable of handling phenomena such as steady-state oscillations and slow convergence under rapidly changing irradiance conditions.

The comparative energy harvesting capability is shown in **Figure 7**, where the average output power obtained in four experimental operation patterns is given. In all cases, the proposed OA-P&O achieves higher average output power than the conventional P&O. This improvement is mainly due to the capacity of the OA-P&O to decrease unnecessary perturbations near the MPP. The dead-band mechanism under steady-state conditions prevents repetitive updates of the duty cycle when the power variation becomes sufficiently small, minimizing oscillation-induced power loss.

Furthermore, the adaptive variable step-size mechanism under dynamic operating conditions provides a faster movement to the new operating point, which further decreases energy waste during irradiance transitions. In the most demanding working pattern, the output power improves from 70.31 W for the traditional P&O to 78.87 W for the proposed OA-P&O, demonstrating a considerable improvement in the energy harvesting capability.

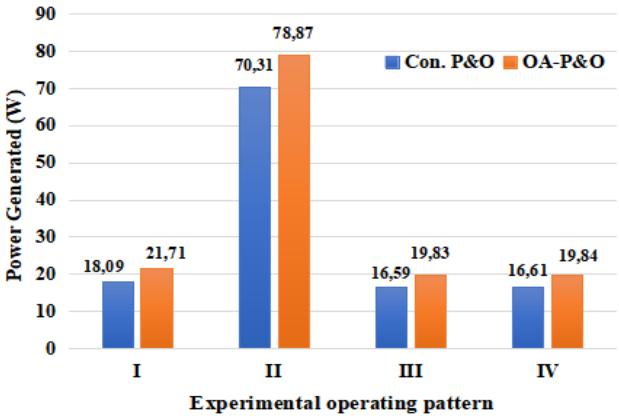


Figure 7. Comparative average power generated under experimental operating pattern

The transient performance of the system is also analysed in the aspect of the tracking speed. The comparison of the PV power stabilisation time between the conventional P&O and the suggested OA-P&O under the transient events is shown in **Figure 8**. The values on the vertical axis represent the time required for the PV power signal to settle following an abrupt shift of irradiance. The results demonstrate that the proposed OA-P&O consistently yields a reduced stabilization time compared to the traditional P&O in all measurable transitions.

This improvement is mainly owed to the adaptive VSS mechanism that alters the perturbation step based on the slope of the *P-V* characteristic. Therefore, the controller speeds up the convergence if the operating point is far away from the MPP, but ensures stable tracking when it approaches the new MPP.

To further position the proposed method within the broader context of P&O-based MPPT developments, **Table 8** presents a comparative feature analysis between the introduced OA-P&O and several representative MPPT methods reported in the literature. The comparison is carried out with respect to several important design characteristics, including variable step-size capability, dead-band implementation, requirement for extra sensors, drift mitigation, and computational complexity.

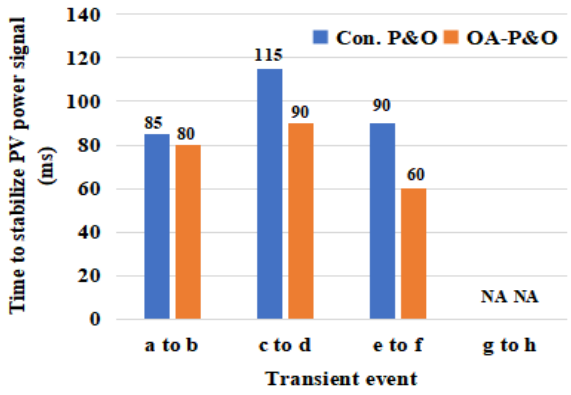


Figure 8. MPPT power stabilization time comparison during transient events

Table 8 positions the proposed OA-P&O relative to representative P&O-based MPPT methods reported in the literature. Unlike the conventional P&O, the proposed method incorporates both adaptive VSS control and dead-band stabilization. Compared with the adaptive VSS approach in [7], which provides only partial drift mitigation through step-size adaptation, the proposed OA-P&O introduces an explicit bounded-slope mechanism to prevent unstable updates when the voltage variation becomes very small. In contrast to the drift-free method [37], which requires additional sensing, the proposed OA-P&O achieves explicit drift mitigation without extra sensors. Therefore, the main advantage of the proposed method lies in integrating adaptive tracking, oscillation suppression, and bounded update behaviour within a structurally simple implementation framework.

Table 8. Comparative feature analysis of various MPPT algorithms

Method	VSS	Dead-band stabilization	Extra sensors	Drift mitigation	Complexity basis
Conventional P&O	×	×	×	None	Basic fixed-step arithmetic
Adaptive VSS P&O [7]	√	×	×	Partial	Adaptive slope evaluation
Drift-free P&O [37]	√	×	√	Explicit	Adaptive logic with additional sensing
Proposed OA-P&O	√	√	×	Explicit	Adaptive logic with dead-band and bounded-slope update

In contrast, the proposed OA-P&O combines three important features within a unified low-complexity framework: adaptive variable step-size control, dead-band stabilization, and bounded slope evaluation for drift mitigation. Unlike the drift-free method in [37], the proposed method does not require extra sensors, and unlike the adaptive VSS method in [7], it explicitly incorporates a dead-band mechanism to suppress unnecessary perturbations near the MPP. Thus, the fundamental contribution of the proposed OA-P&O is not only the introduction of another adaptive perturbation approach but also the realistic implementation of fast tracking, oscillation suppression and computational robustness without noticeably raising the implementation overhead.

The comparison indicates that the suggested OA-P&O can be regarded as a feasible compromise between simplicity of implementation and better MPPT performance. It maintains the structural simplicity of the P&O with the addition of sufficient adaptive intelligence to improve both transient and steady state performance under rapidly fluctuating irradiance conditions. The results also reveal that the suggested OA-P&O surpasses the conventional P&O in terms of harvested power, steady-state stability and transient tracking speed.

It is worth acknowledging certain operation boundaries of the proposed OA-P&O controller, particularly under complex atmospheric scenarios. While the algorithm effectively minimizes steady-state oscillations and accelerates tracking speed under uniform irradiance shifts, its reliance on local gradient updates $\left(\frac{\Delta P}{\Delta V}\right)$ presents challenges during Partial Shading Conditions (PSC). In such non-uniform environments, the *P-V* curve develops multiple local peaks. Without a global scanning mechanism or stochastic optimization routine, local gradient-based methods like OA-P&O can become trapped at a local maximum power point if the initial operating state lies within its catchment zone. Addressing multi-peak tracking under severe shading without inflating computational complexity remains an open direction for future integration.

CONCLUSION

The proposed Optimised Adaptive P&O (OA-P&O) algorithm aims to eliminate the main drawback of the conventional P&O approach especially steady state power oscillation and slow convergence under rapidly fluctuating irradiance. The suggested method combines adaptive variable step-size control, dead-band stabilisation and bounded slope computation mechanism with a low-complexity framework.

The results demonstrated that this method is able to enhance the MPPT performance in two crucial aspects. First, the dead-band technique is able to eliminate unnecessary perturbations around the MPP and minimises steady-state oscillation. Secondly, the constrained slope calculation results in more robust calculations by preventing unstable updates as the voltage fluctuation tends to zero. Experimental validation showed that the suggested technique delivers faster stabilisation, smaller ripple, and higher collected power in comparison with the standard P&O for all the investigated operating patterns.

Overall, the OA-P&O offers a practical improvement over the conventional P&O without requiring additional sensors or significantly increasing implementation complexity. Finally, while the hardware-in-the-loop (HIL) experimental results confirmed the efficacy of the proposed OA-P&O algorithm across four representative dynamic scenarios, real-word outdoor field test under unconstrained and continuous meteorological fluctuations were not conducted. Testing twin parallel physical PV setup under natural outdoor conditions presents a high valuable avenue for future research to further validate long-term operational durability and energy harvest gains under actual environmental dynamics. Additionally, future work should investigate its performance under partial shading conditions and explore AI-based adaptive turning for further enhancement

ACKNOWLEDGMENT(S)

This research was supported by Directorat Penelitian dan Pengabdian Kepada Masyarakat, Directorat Jendral Riset dan Pengembangan, Kementerian Pendidikan Tinggi, Sains dan Teknologi. Contract No. 088/C3/DT.05.00/PL/2025.

NOMENCLATURE

Abbreviations

MPPT	Maximum Power Point Tracking
MPP	Maximum Power Point
OA-P&O	Optimized Adaptive-Perturb and Observe
PV	Photovoltaic
P&O	Perturb and Observe
VSS	Variable Step Size

REFERENCES

1. H. H. Pourasl, R. V. Barenji, and V. M. Khojastehnezhad, “Solar energy status in the world: A comprehensive review,” *Energy Reports*, vol. 10, pp. 3474–3493, Nov. 01, 2023, https://doi.org/10.1016/j.egyr.2023.10.022.
2. A. Asnil, R. Nazir, K. Krismadinata, and M. Nasir, “Improved MPPT Performance of VSS-Based Incremental Conductance with Auxiliary PID Correction for Photovoltaic Power Optimization,” *Mathematical Modelling of Engineering Problems*, vol. 12, no. 7, pp. 2417–2426, 2025, https://doi.org/10.18280/mmep.120720.
3. L. Guanghua, A. M. Soomar, S. H. H. Shah, S. Shaikh, and P. Musznicki, “Maximum Power Point Tracking Strategies for Solar PV Systems: A Review of Current Methods and Future Innovations,” *Results in Engineering*, Art.no. 107227, Sep. 2025, https://doi.org/10.1016/j.rineng.2025.107227.

4. T. Sutikno, A. C. Subrata, and M. H. Jopri, "Milestone of the most used maximum power point tracking in solar harvesting system," *International Journal of Power Electronics and Drive Systems*, vol. 13, no. 3, 2022, https://doi.org/10.11591/ijpeds.v13.i3.pp1277-1284.
5. D. Sibtain, M. M. Gulzar, K. Shahid, I. Javed, S. Murawwat, and M. M. Hussain, "Stability Analysis and Design of Variable Step-Size P&O Algorithm Based on Fuzzy Robust Tracking of MPPT for Standalone/Grid Connected Power System," *Sustainability (Switzerland)*, vol. 14, no. 15, Aug. 2022, https://doi.org/10.3390/su14158986.
6. A. Aurairat and B. Plangklang, "An alternative perturbation and observation modifier maximum power point tracking of PV systems," *Symmetry (Basel).*, vol. 14, no. 44, pp. 1–17, 2022, https://doi.org/10.3390/sym14010044.
7. M. Gopahanal Manjunath, C. Vyjayanthi, and C. N. Modi, "Adaptive step size based drift-free P&O algorithm with power optimiser and load protection for maximum power extraction from PV panels in stand-alone applications," *IET Renewable Power Generation*, vol. 15, no. 6, pp. 1270–1285, 2021, https://doi.org/10.1049/rpg2.12105.
8. M. Ahmed, M. Abdelrahem, I. Harbi, and R. Kennel, "An adaptive model-based MPPT technique with drift-avoidance for grid-connected PV systems," *Energies (Basel).*, vol. 13, no. 24, 2020, https://doi.org/10.3390/en13246656.
9. A. Saberi, M. Niroomand, and B. M. Dehkordi, "An Improved P&O Based MPPT for PV Systems with Reduced Steady-State Oscillation," *Int. J. Energy Res.*, vol. 2023, 2023, https://doi.org/10.1155/2023/4694583.
10. A. Chellakhi, S. El Beid, and Y. Abouelmahjoub, "An improved adaptable step-size P&O MPPT approach for standalone photovoltaic systems with battery station," *Simul. Model. Pract. Theory*, vol. 121, Dec. 2022, https://doi.org/10.1016/j.simpat.2022.102655.
11. J. M. Riquelme-Dominguez and S. Martinez, "Comparison of Different Photovoltaic Perturb and Observe Algorithms for Drift Avoidance in Fluctuating Irradiance Conditions," 2020, https://doi.org/10.1109/EEEIC/ICPSEurope49358.2020.9160791.
12. M. A. Yildirim and M. Nowak-Ocłoń, "Modified maximum power point tracking algorithm under time-varying solar irradiation," *Energies (Basel).*, vol. 13, no. 24, Dec. 2020, https://doi.org/10.3390/en13246722.
13. A. Chellakhi, S. El Beid, M. El Marghichi, E. M. Bouabdalli, A. Harrison, and H. Abouobaida, "Implementation of a low-cost current perturbation-based improved PO MPPT approach using Arduino board for photovoltaic systems," *e-Prime - Advances in Electrical Engineering, Electronics and Energy*, vol. 10, 2024, https://doi.org/10.1016/j.prime.2024.100807.
14. H. Alhusseini, M. Niroomand, and B. M. Dehkordi, "A Fuzzy-Based Adaptive P&O MPPT Algorithm for PV Systems With Fast Tracking and Low Oscillations Under Rapidly Irradiance Change Conditions," *IEEE Access*, vol. 12, pp. 84374–84386, 2024, https://doi.org/10.1109/ACCESS.2024.3412848.
15. B. Cruz, L. Ricalde, R. Quintal-Palomo, A. Bassam, and R. I. Rico-Camacho, "Hybrid Artificial Neural Network and Perturb & Observe Strategy for Adaptive Maximum Power Point Tracking in Partially Shaded Photovoltaic Systems," *Energies (Basel).*, vol. 18, no. 19, 2025, https://doi.org/10.3390/en18195053.
16. M. Yilmaz, "Comparative Analysis of Hybrid Maximum Power Point Tracking Algorithms Using Voltage Scanning and Perturb and Observe Methods for Photovoltaic Systems under Partial Shading Conditions," *Sustainability (Switzerland),* vol. 16, no. 10, 2024, https://doi.org/10.3390/su16104199.
17. A. T. Naser, N. F. Ab Aziz, K. K. Mohammed, K. Binti Kamil, and S. Mekhilef, "A novel hybrid GMPPT method for PV systems to mitigate power oscillations and partial shading detection," *Renew. Energy*, vol. 237, Dec. 2024, https://doi.org/10.1016/j.renene.2024.121520.

18. O. A. Ba, A. Ndiaye, A. Ba, E. H. M. Ndiaye, and M. A. Tankari, "Optimization of the P&O-MPPT controller by the adaptive method (Ad-P&O) for stand-alone PV systems," 2023, https://doi.org/10.1109/icSmartGrid58556.2023.10171074.
19. A. B. Djilali *et al.*, "Enhanced variable step sizes perturb and observe MPPT control to reduce energy loss in photovoltaic systems," *Sci. Rep.*, vol. 15, no. 1, Dec. 2025, https://doi.org/10.1038/s41598-025-95309-y.
20. R. I. Rico-Camacho, L. J. Ricalde, A. Bassam, M. I. Flota-Bañuelos, and A. Y. Alanis, "Transient Differentiation Maximum Power Point Tracker (Td-MPPT) for Optimized Tracking under Very Fast-Changing Irradiance: A Theoretical Approach for Mobile PV Applications," *Applied Sciences (Switzerland)*, vol. 12, no. 5, 2022, https://doi.org/10.3390/app12052671.
21. A. Harrison, E. M. Nfah, J. De Dieu Nguimfack Ndongmo, and N. H. Alombah, "An Enhanced P&O MPPT Algorithm for PV Systems with Fast Dynamic and Steady-State Response under Real Irradiance and Temperature Conditions," *International Journal of Photoenergy*, vol. 2022, 2022, https://doi.org/10.1155/2022/6009632.
22. M. L. Katche, A. B. Makokha, S. O. Zachary, and M. S. Adaramola, "A Comprehensive Review of Maximum Power Point Tracking (MPPT) Techniques Used in Solar PV Systems," *Energies*, vol. 16, no. 5. MDPI, Mar. 01, 2023, https://doi.org/10.3390/en16052206.
23. G. Prabowo, S. D. Nugraha, F. H. Sholihah, E. Sunarno, and M. D. Hanamsyah, "Enhancing PV Maximum Power Point Tracking in Residential Charging Stations through Variable Step Size Modification in P&O Algorithm," 2023, https://doi.org/10.1109/IEIT59852.2023.10335576.
24. E. P. Sarika, J. Jacob, S. Sheik Mohammed, and S. Paul, "Standalone PV system with modified VSS P&O MPPT controller suitable for partial shading conditions," in *Proceedings of the 7th International Conference on Electrical Energy Systems, ICEES 2021*, Feb. 2021, pp. 51–55, https://doi.org/10.1109/ICEES51510.2021.9383697.
25. M. Ahmed, I. Harbi, C. M. Hackl, R. Kennel, J. Rodriguez, and M. Abdelrahem, "Maximum power point tracking-based model predictive control with reduced sensor count for PV applications," *IET Renewable Power Generation*, vol. 19, no. 1, 2025, https://doi.org/10.1049/rpg2.12535.
26. K. Ullah, M. Ishaq, F. Tchier, H. Ahmad, and Z. Ahmad, "Fuzzy-based maximum power point tracking (MPPT) control system for photovoltaic power generation system," *Results in Engineering*, vol. 20, Dec. 2023, https://doi.org/10.1016/j.rineng.2023.101466.
27. R. B. Roy *et al.*, "A Comparative Performance Analysis of ANN Algorithms for MPPT Energy Harvesting in Solar PV System," *IEEE Access*, vol. 9, 2021, https://doi.org/10.1109/ACCESS.2021.3096864.
28. J. S. Koh, R. H. G. Tan, W. H. Lim, and N. M. L. Tan, "A Modified Particle Swarm Optimization for Efficient Maximum Power Point Tracking Under Partial Shading Condition," *IEEE Trans. Sustain. Energy*, vol. 14, no. 3, 2023, https://doi.org/10.1109/TSTE.2023.3250710.
29. A. Almalaq, A. Harrison, I. Alsaleh, A. Alassaf, and M. Alangari, "Comprehensive control strategy for standalone photovoltaic systems with integrated optimum power harvesting and voltage regulation through microcontroller in the loop experimentation," *Sci. Rep.*, vol. 15, no. 1, 2025, https://doi.org/10.1038/s41598-025-24134-0.
30. S. J. Yaqoob *et al.*, "Advanced Maximum Power Point Tracking in Photovoltaic Systems: A Comprehensive Review of Classical, AI-Based, and Metaheuristic Optimization Techniques," *Engineering Reports*, vol. 7, no. 9. John Wiley and Sons Inc, Sep. 01, 2025, https://doi.org/10.1002/eng2.70404.

31. A. Elsafi, A. A. Almohammedi, M. Balfaqih, Z. Balfagih, and S. Sabri, "Comparative analysis of maximum power point tracking methods for power optimization in grid tied photovoltaic solar systems," *Discover Applied Sciences*, vol. 7, no. 9, Sep. 2025, https://doi.org/10.1007/s42452-025-07606-w.
32. A. Ali *et al.*, "Review of online and soft computing maximum power point tracking techniques under non-uniform solar irradiation conditions," *Energies (Basel).*, vol. 13, no. 12, pp. 1–37, Jun. 2020, https://doi.org/10.3390/en13123256.
33. F. Liu, S. Duan, F. Liu, B. Liu, and Y. Kang, "A variable step size INC MPPT method for PV systems," *IEEE Transactions on Industrial Electronics*, vol. 55, no. 7, pp. 2622–2628, Jul. 2008, https://doi.org/10.1109/TIE.2008.920550.
34. G. Nadia and B. H. Mouna, "Boost DC–DC Converter with MPPT for PV Application," in *Proceedings of the 2nd International Conference on Green Energy Conversion System. ICGECS 2023. Green Energy and Technology*, Nov. 2024, pp. 181–194, https://doi.org/10.1007/978-981-97-6148-7_17.
35. A. Raj and R. P. Praveen, "Highly efficient DC-DC boost converter implemented with improved MPPT algorithm for utility level photovoltaic applications," *Ain Shams Engineering Journal*, vol. 13, no. 3, May 2022, https://doi.org/10.1016/j.asej.2021.10.012.
36. S. Motahhir, A. El Ghzizal, S. Sebti, and A. Derouich, "MIL and SIL and PIL tests for MPPT algorithm," *Cogent Eng.*, vol. 4, no. 1, Jan. 2017, https://doi.org/10.1080/23311916.2017.1378475.
37. M. Buyuk and M. Inci, "Improved drift-free P&O MPPT method to enhance energy harvesting capability for dynamic operating conditions of fuel cells," *Energy*, vol. 267, Mar. 2023, https://doi.org/10.1016/j.energy.2022.126543.

